Article

Uric Acid Inhibits Mice Pancreatic Steatosis via the Glycerophospholipid Pathway

Yang Xiao, Lina Han, Han Wang, Helin Ke, Shaodan Xu, Zhibin Huang, Guorong Lyu,* and Shilin Li*

Cite This: *ACS Omega* 2024, 9, 21829−21837

Read Online

ACCESS | Metrics & More | Article Recommendations | SI Supporting Information

ABSTRACT: *Background*: despite evidence for mutually reinforcing effects of serum uric acid (SUA) and lipids, the effects of uric levels on pancreatic steatosis are not well-established. In this study, the relationship between low concentrations of uric acid and pancreatic steatosis was evaluated. *Methods*: forty C57BL/6J mice were fed a diet of high uric acid (HU), high fat (HF), high uric acid and high fat (HUHF), and normal control (NC) (10 mice in each group). Weight was measured weekly. Ultrasonography was performed to observe the pancreatic echo intensity of all mice before the end of feeding. Subsequently, peripheral blood was taken for biochemical examination. Intact pancreatic tissues were taken, part of which was used for pathological examination, part of which was used for PCR experiments and Western Blot experiments to obtain glycerophospholipid-associated mRNA data and protein levels. *Results*: body weight was significantly higher in the HF group than in the other three groups. Higher uric acid matched lower total cholesterol and triglyceride, matched higher low-density lipoprotein, and matched equal high-density lipoprotein. Ultrasound images and HE staining of pancreatic tissues of mice showed that higher uric acid matched lower fat content. The mRNA levels of phospholipase A2 group IB were highest in high uric acid group, while relative protein expression levels were lowest in high uric acid and control groups. Phospholipase A2 group IIA showed the opposite patterns. *Conclusions*: elevated serum uric acid at low concentrations can inhibit pancreatic steatosis, which is modulated via the glycerophospholipid metabolic pathway.
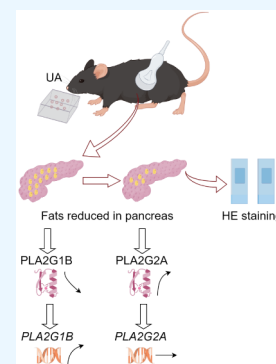
INTRODUCTION

Obesity has gradually become an important issue affecting human health. Based on a study involving 195 countries, the obese population in 2015 exceeded 600 million, and the childhood obesity population exceeded 100 million. The obese population has doubled since 1980, with a continuing upward trend.[1] Obesity can lead to an increased risk of cardiovascular disease, diabetes,[2] and even cancer.[3] When body fat increases beyond the storage capacity of the adipose tissue, it is stored in nonadipose organs, such as the liver and pancreas.[4] Pancreatic steatosis (PS) was originally described in 1933.[5] Increasing evidence suggests that PS is associated with type 2 diabetes, metabolic syndrome, atherosclerosis, acute severe pancreatitis, and pancreatic cancer.[6,7] PS can be an initial indicator of "ectopic fat deposition," which occurs before nonalcoholic fatty liver disease.[5] Intrapancreatic fat deposits are a precursor to pancreatic cancer in patients with pancreatitis.[8] Mean lipid and uric acid levels are significantly higher in patients with PS than in patients without PS.[9] The prevalence of PS is elevated in patients with hyperlipidemia.[10] However, it is not clear whether hyperuricemia affects PS.

In a large-scale health and nutrition survey, patients with hyperuricemia were 2.46 times more likely to develop heart failure than the general population, and all-cause mortality was 1.37 times higher in these patients. Serum uric acid (SUA) levels were nonlinearly correlated with all-cause mortality, with a negative correlation when the SUA level was less than 300 μmol/L and a significant positive correlation when the SUA

level was more than 300 μmol/L.[11] Several studies have reported a positive association between uric levels and venous thromboembolism,[12,13] whereas a more recent study has shown that there is no obvious causal relationship between uric levels and venous thromboembolism under a linear relationship assumption between them. However, other non-linear relationships, such as U-shaped relationship, are still a possibility.[14] High uric acid levels can cause inflammation and oxidative stress, promote the death of pancreatic β-cells,[15] and induce diabetes in male mice.[16] However, an appropriate increase in uric acid at low concentrations may improve short-term functional outcomes of ischemic stroke in patients with type 2 diabetes[17] and reduce the risk of death associated with prostate cancer.[18] Moreover, at physiological concentrations, uric acid acts as an antioxidant,[19−23] scavenging oxygen radicals and exerting a protective effect on most organs,[19,22] except the nervous system.[22] Several studies have shown that low uric acid levels damage the nervous system,[24,25] whereas high uric acid levels exert protective effects.[26] Many studies have suggested that high-fat diets cause elevated uric acid levels in addition to
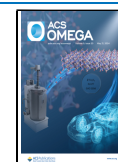
elevated blood lipids.[27−29] Moreover, a high uric acid diet causes elevated blood lipids.[30,31] These results confirm that there is a mutual promotion between uric acid and blood lipids.[32] However, it is not clear whether high uric acid combined with high lipid levels has a reinforcing effect on PS.

Glycerophospholipids, the most abundant type of phospholipids in organisms, are involved in the recognition of proteins and signaling in cell membranes, in addition to constituting biological membranes. Glycerophospholipids play an important role in biological processes and are an important predictive indicator of the physiological and pathological states of an organism.[33] Glycerophospholipids can produce many derivatives via various enzymes, the most important of which is phospholipase A2 (PLA2), which belongs to a superfamily of phospholipase enzymes. Under physiological conditions, PLA2 is involved in phospholipid remodeling, cytokinesis, neurotransmitter release, and the regulation of several lipid second messengers. PLA2 group IB (PLA2G1B) and PLA2 group IIA (PLA2G2A) are secretory enzymes. PLA2G1B levels are high in the pancreas and are associated with obesity, hyperglycemia, insulin resistance, and hyperlipidemia,[34] whereas PLA2G2A prevents weight gain and insulin resistance.[35,36] However, the role of the glycerophospholipid pathway in PS is not well established.

We hypothesized that at physiological concentrations, uric acid attenuates PS. To evaluate this hypothesis, we established a mouse model of PS and evaluated the effects of uric acid on lipids, PS, and glycerophospholipid metabolism-related genes and proteins. The results of this study provide a basis for the development of strategies to delay or even stop the progression of PS and provide potential targets for prevention and treatment.

■ MATERIALS AND METHODS

Preparation of Animal Feed. The essential nutrients for common feed are as follows: crude protein 19.2%, crude fat 4.6%, crude fiber 4.0%, crude ash 6.3%, moisture 8.8%, calcium 1.19%, and total phosphorus 0.87%. Its energy supply ratios are 22.47% for protein, 12.11% for fat, and 65.42% for carbohydrates. More detailed parameters are described in Figure S1. High uric acid feed included potassium oxonate (3% by mass) and yeast powder (20% by mass) in the common feed. High-fat feed included a 60% fat−calorie ratio and 35% mass ratio (derived from lard and soybean oil (10:1)); the remaining ingredients were the same as those in the common feed. High uric acid and high-fat feed contained potassium oxonate (3% by mass), yeast powder (20% by mass), 60% fat calorie ratio, and 35% mass ratio (derived from lard and soybean oil (10:1)) in the common feed. Potassium oxonate was provided by Shanghai Yi En Chemical Technology Co., Ltd., and the remaining raw materials and feed were produced and provided by Jiangsu Synergy Bioengineering Co., Ltd.

Animal Modeling. Forty healthy C57BL/6J male mice, 12 weeks old, weighing 21.11−30.20 g, were provided by the Zhejiang Weitonglihua Laboratory Animal Technology Co., Ltd. (License No.: SCXK (Zhejiang) 2019-0001, Certificate of Conformity No.: 20221103Abzz0619000469). The mice were housed at the Laboratory Animal Centre of Quanzhou Medical College (Laboratory Animal Use Permit No. SYXK (Min) 2016-0001). After 1 week of acclimatization, the mice were randomly divided into four groups: HU group (high uric acid feed), HF group (high-fat feed), HUHF group (high uric acid and high-fat feed), and NC group (common feed). The mice were placed in cages with a similar size, shape, and height of bedding and

maintained for 12 weeks. The body weight was monitored weekly during the study period. The mice were allowed ad libitum access to food and water and maintained at 19−23 °C, humidity of 58−65%, and a 12 h light−dark cycle. The animal study protocol was approved by the Ethics Committee of The Second Affiliated Hospital of Fujian Medical University (protocol code 231; approval date: 2022).

Acquisition and Analysis of Ultrasound Images. The pancreas of each mouse was scanned using an L20 line array probe (frequency 20 MHz) of the Resona 7 color Doppler ultrasound diagnostic instrument (Mindray, Shenzhen, China) 1−2 days before the end of rearing.

All mice used for ultrasonography were fasted and dehydrated for 24 h. The mice were anaesthetized with an intraperitoneal injection of 2% pentobarbital sodium solution (0.003 mL/g). The left abdominal hair of each mouse was removed, the limbs were fixed, and after applying an appropriate amount of couplant, the probe was placed in the direction of the long axis of the mouse spleen (Figure 1A). The pancreas was located in the left upper part of the mouse abdomen (Figure 1B,C). All mice underwent ultrasonography and resumed eating and drinking for at least 1 day.
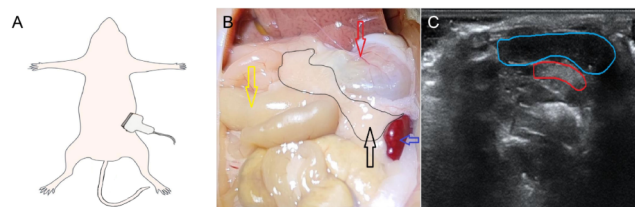

Figure 1. Schematic diagrams of the manipulation for scanning the mouse pancreas. (A) Model diagram, the high-frequency probe is placed on the left upper abdomen at an approximately 30-degree angle to the long axis of the mouse. (B) Anatomic diagram; the liver is raised upward, and the pancreas (black arrow) is a pale yellow structure located between the stomach (red arrow), spleen (blue arrow), and intestine (yellow arrow). (C) Ultrasonogram, the pancreas (red circle) is uniformly and moderately echogenic and located deep in the spleen (blue circle).

After the pancreatic ultrasound images of all mice were acquired, they were uniformly imported into ImageJ to extract the average gray value of the pancreatic echo intensity (PEI) and simultaneously extract the average gray value of the spleen echo intensity (SEI) at the same level. The gray value of PEI was subtracted from the gray value of SEI[9,10] to obtain a calibrated and relatively accurate gray value. The region of interest (ROI) was within the pancreas or spleen; three homogeneous locations were measured separately, and the average value was obtained (Figure 2) for the final pancreatic echo intensity (fPEI). The effects of blood vessels, fat, and gastric contents on PEI were avoided as much as possible.

Collection of Animal Specimens. At the end of the feeding period, all mice were fasted for 24 h with appropriate water. Anaesthesia was induced by an intraperitoneal injection of 2% sodium pentobarbital solution at 0.003 mL/g. Blood was obtained using the eyeball removal method and stored in EP tubes for the determination of relevant biochemical data. Pancreatic tissues were rapidly isolated by laparotomy. One part was fixed in 10% buffered formalin solution for 24−48 h for HE staining, and the other part was quick-frozen in liquid nitrogen and then rapidly transferred to a −80 °C refrigerator for
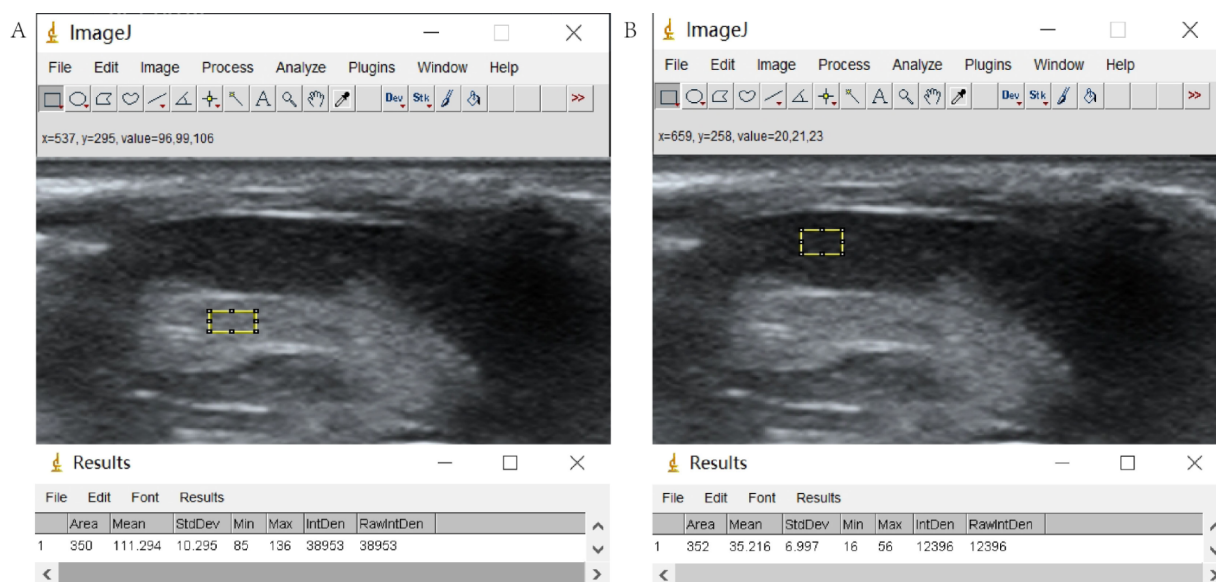
Figure 2. Schematic diagrams of grayscale sampling. (A) Sampling manipulation for the pancreas. (B) Sampling manipulation for the spleen.
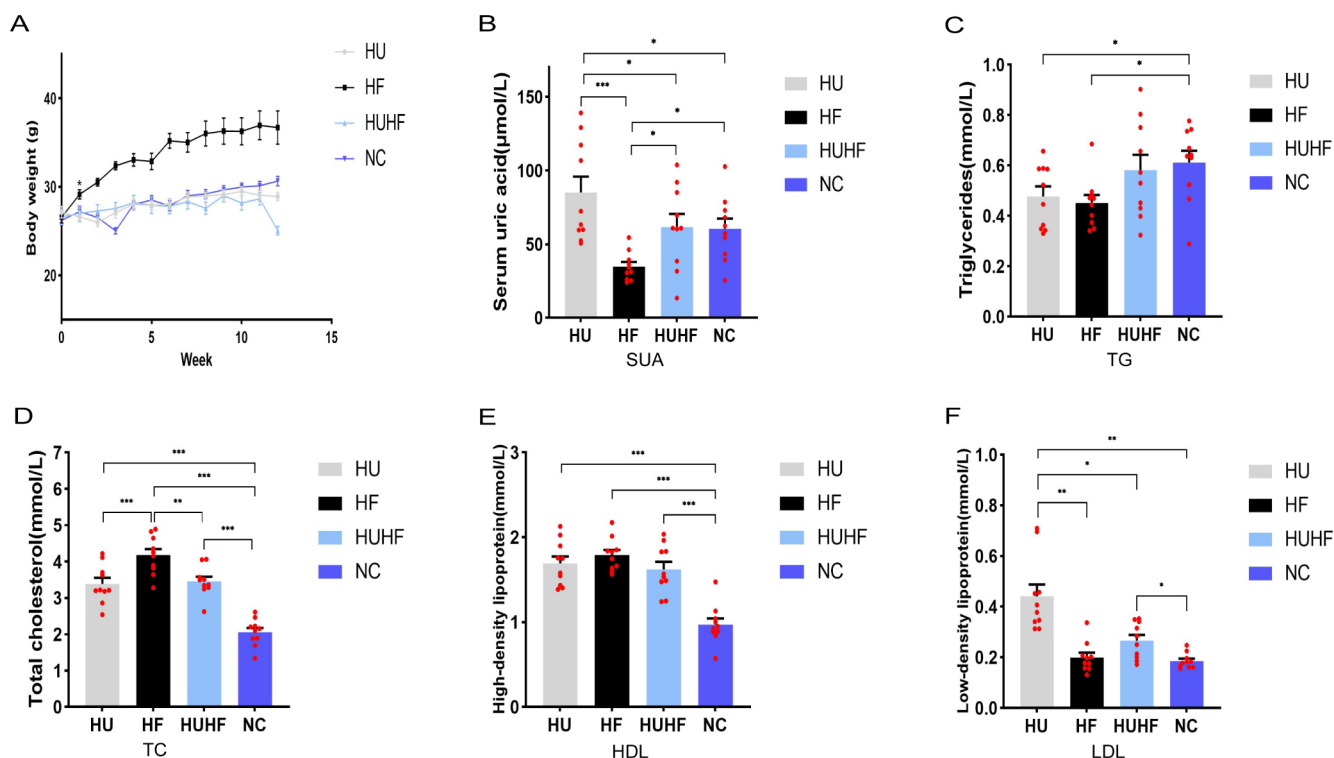

Figure 3. Body weights and blood biochemical parameters. (A) Body weight, (B) SUA, (C) TG, (D) TC, (E) HDL, (F) LDL for each group. HU: high uric acid; HF: high fat; HUHF: high uric acid and high fat; NC: normal control; SUA: serum uric acid; TG: triglyceride; TC: total cholesterol; HDL: high-density lipoprotein; LDL: low-density lipoprotein. $*p < 0.05$; $** p < 0.01$; $*** p < 0.001$.

quantitative reverse transcriptase-polymerase chain reaction (qRT-PCR) and Western blot experiments.

Blood Biochemistry. The blood of mice stored in EP tubes was centrifuged (3000 rpm, 15 min), and the supernatant was extracted for the determination of SUA, TC, TG, HDL, and LDL.

Histopathological Examination. The fixed pancreatic tissues were sequentially dehydrated, paraffin-embedded, and sectioned at a thickness of 4 μm for histological examination by HE staining and observations under a light microscope (Nikon,

Tokyo, Japan). The criteria[37,38] for hepatic steatosis were modified to obtain a PS rating scale (Table S1).

Two spaced sections of the pancreatic tissue were obtained from each mouse, with two fields of view in one section, each of which was equally divided into nine ROIs and scored according to the criteria described above. The total scores for all ROIs were summed, the average score for each specimen (36 ROIs) was calculated, and the same method was applied to the pancreatic tissues of the remaining mice. The final scores for all mice were pooled to compare the degree of PS in each group.

Table 1. Data of Mice in Four Groups[ab]

	HU	HF	HUHF	NC	F value	P value
Section A						
body weight (g)	26.67 (0.48)	30.53 (0.43)	26.63 (0.79)	26.53 (0.46)	12.380	<0.001
SUA (μmol/L)	84.83 (10.88)	34.78 (9.72)	61.60 (8.87)	60.44 (6.94)	6.569	0.001
TG (mmol/L)	0.48 (0.04)	0.45 (0.03)	0.58 (0.06)	0.61 (0.05)	2.906	0.048
TC (mmol/L)	3.39 (0.17)	4.18 (0.17)	3.46 (0.13)	2.06 (0.12)	36.165	<0.001
HDL (mmol/L)	1.69 (0.08)	1.79 (0.06)	1.62 (0.09)	0.97 (0.07)	23.125	<0.001
LDL (mmol/L)	0.44 (0.05)	0.20 (0.02)	0.27 (0.02)	0.19 (0.01)	17.775	<0.001
Section B						
fPEI	72.24 (4.70)	80.60 (5.06)	57.44 (5.62)	30.59 (2.12)	23.019	<0.001
pathological scores	0.98 (0.03)	1.03 (0.02)	0.77 (0.02)	0.38 (0.02)	205.108	<0.001
Section C						
PLA2G1B (mRNA)	5.97 (0.59)	2.33 (0.74)	3.66 (0.81)	2.44 (0.76)	5.384	0.004
PLA2G2A (mRNA)	1.72 (0.23)	1.69 (0.47)	1.51 (0.54)	1.55 (0.29)	0.658	0.583
PLA2G1B (protein)	0.29 (0.04)	0.91 (0.06)	0.84 (0.07)	0.18 (0.05)	46.521	<0.001
PLA2G2A (protein)	0.91 (0.07)	0.37 (0.12)	0.38 (0.22)	0.54 (0.13)	4.880	0.007

[a]Data are expressed as mean (SD or SEM). [b]Abbreviations: HU: high uric acid; HF: high fat; HUHF: high uric acid and high fat; NC: normal control; SUA: serum uric acid; TG: triglyceride; TC: total cholesterol; HDL: high-density lipoprotein; LDL: low-density lipoprotein; fPEI: final pancreatic echo intensity.
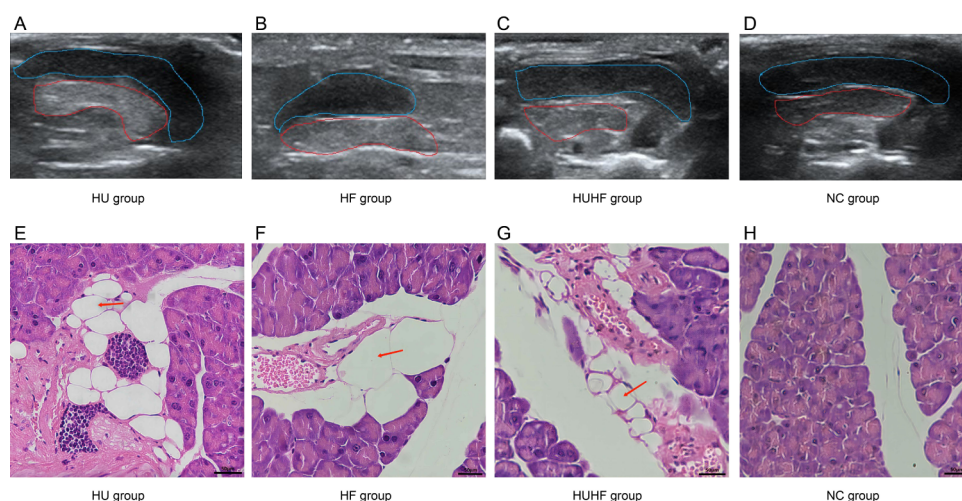

Figure 4. Ultrasonogram of the pancreas and spleen and HE-stained sections of the pancreas in each group. (A−D) Ultrasonogram of the pancreas and spleen of HU, HF, HUHF, and NC groups. The pancreas (red circle) is a higher echo and located deep in the spleen (blue circle). (E−H) HE-stained sections of the pancreas of the HU, HF, HUHF, and NC groups. The fat droplets in the HU and HF groups were large (red arrows) and partially fused, while the fat droplets in the HUHF group were small (red arrow). There were no obvious fat droplets in NC group. HU: high uric acid; HF: high fat; HUHF: high uric acid and high fat; NC: normal control.

Detection of *PLA2G1B* and *PLA2G2A* mRNA Levels Using qRT-PCR. The mRNA levels of *PLA2G1B* and *PLA2G2A* in mouse pancreatic tissues were detected by qRT-PCR, according to the instructions provided with the reverse transcription kit and qPCR operation manual (Servicebio Ltd., Hubei, China). The primer sequences are shown in Table S2. Total RNA was extracted using TRIzol reagent, and RT-PCR was performed after reverse transcription. PCR was carried out using a 20 μL reaction system with the following steps: predenaturation at 95 °C for 30 s, denaturation at 95 °C for 15 s, annealing at 60 °C for 30 s, and extension at 60 °C for 30 s, with 40 cycles in total. Normalized expression levels were determined and standardized against *GAPDH* levels.

Western Blotting. The pancreatic tissue was lysed in RIPA lysis buffer and centrifuged for 10 min (12,000 rpm, 4 °C). The protein concentration was then quantified. Protein lysates (10 mL) were analyzed using sodium dodecyl sulfate-polyacrylamide gel electrophoresis (SDS-PAGE), followed by electro-transfer onto PVDF membranes (Servicebio Ltd.). The membranes were blocked with 5% skim milk powder and incubated with anti-PLA2G1B (16 kDa; 1:1000) (Servicebio Ltd.), anti-PLA2G2A (16 kDa; 1:1000) (Affinity Biosciences, Jiangsu Parent Biology Research Center Ltd., China), and anti-β-actin (42 kDa; 1:1000) (Servicebio Ltd.) at 4 °C overnight, followed by incubation with the horseradish peroxidase (HRP)-conjugated (rabbit) secondary antibody for 30 min at room temperature. Finally, the samples were visualized using enhanced chemiluminescence (ECL) (Servicebio Ltd.) on a chemiluminescence instrument (6100; CLINX, Shanghai, China). Densitometric analyses were performed using ImageJ, and relative protein expression levels were calculated by comparison with controls (Servicebio Ltd.).

Statistical Analyses. SPSS 26.0 was used for statistical analyses. Continuous variables with normal distribution were presented as means (standard deviations or standard errors). One-way analysis of variance (ANOVA) was used to compare
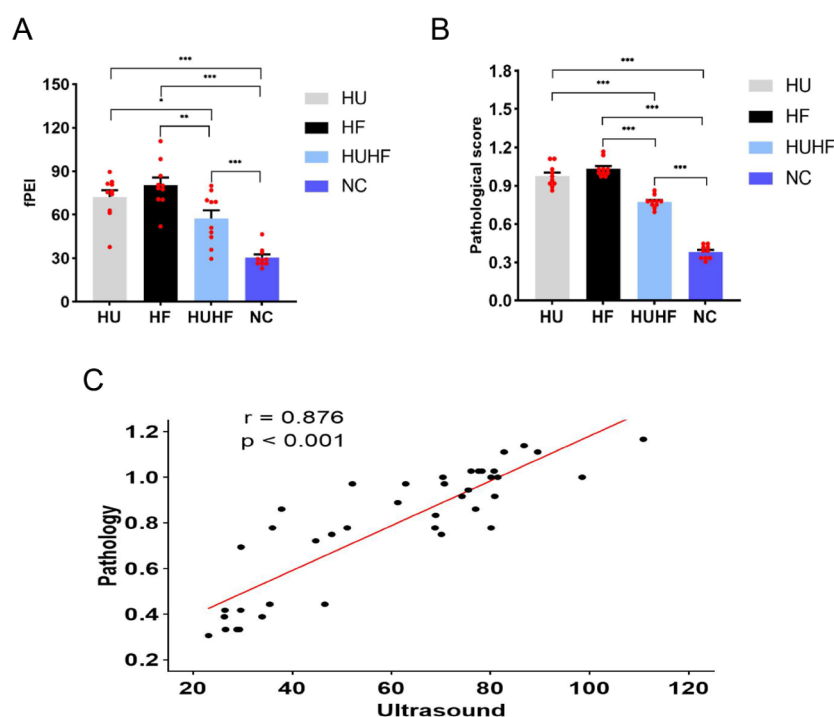
Figure 5. Comparisons of (A) fPEI and (B) pathological score as well as (C) the Pearson's correlation coefficients for the two parameters. HU: high uric acid; HF: high fat; HUHF: high uric acid and high fat; NC: normal control; fPEI = PEI − SEI; PEI: pancreatic echo intensity; SEI: splenic echo intensity; fPEI: final pancreatic echo intensity. * $p < 0.05$; ** $p < 0.01$; *** $p < 0.001$.

mean values among multiple groups. When the variances were homogeneous, the least significant difference (LSD) test was used; otherwise, Dunnett's T3 test was used. Pearson's correlation analysis was used to compare the pathology scores and ultrasound results. Differences were considered statistically significant at $p < 0.05$.

RESULTS

As shown in Figure 3A and Table 1 Section A, from week 1, the body weight of mice in the HF group [30.53 (0.43) g] was significantly higher than those in the HU [26.67 (0.48) g], HUHF [26.63 (0.79) g], and NC groups [26.53 (0.46) g] ($F = 12.380$, $p < 0.001$). Blood biochemical data (Figure 3B−F and Table 1 Section A) showed that the SUA levels in the HUHF group [61.60 (8.87) μmol/L] and NC group [60.44 (6.94) μmol/L] were significantly lower than that of the HU group [84.83 (10.88) μmol/L] but higher than that of the HF group [34.78 (9.72) μmol/L] ($F = 6.569$, $p = 0.001$). The triglyceride (TG) levels of the HU group [0.48 (0.04) mmol/L] and the HF group [0.45 (0.03) mmol/L] were lower than those of the NC [0.61 (0.05) mmol/L] and HUHF groups [0.58 (0.06) mmol/L] but the differences were not significant (F = 2.906, $p = 0.048$). The total cholesterol (TC) of the HUHF group [3.46 (0.13) mmol/L] and the HU group [3.39 (0.17) mmol/L] was significantly lower than that of the HF group [4.18 (0.17) mmol/L] but higher than that of the NC group [2.06 (0.12) mmol/L] ($F = 36.165$, $p < 0.001$). High-density lipoprotein (HDL) levels in the HU group [1.69 (0.08) mmol/L], HF group [1.79 (0.06) mmol/L], and HUHF group [1.62 (0.09) mmol/L] were significantly higher than that in the NC group [0.97 (0.07) mmol/L] ($F = 23.125$, $p < 0.001$). Low-density lipoprotein (LDL) levels of the HUHF group [0.27 (0.02) mmol/L] were significantly lower than those in the HU group [0.44 (0.05) mmol/L] and higher than those in the NC group

[0.19 (0.01) mmol/L] but not significantly different from those in the HF group [0.20 (0.02) mmol/L] ($F = 17.775$, $p < 0.001$).

As shown in Figures 4A−D and 55A and Table 1 Section B, the final pancreatic echo intensity (fPEI) in the HUHF group [57.44 (5.62)] was significantly lower than those in the HU [72.24 (4.70)] and HF groups [80.60 (5.06)] but higher than that in the NC group [30.59 (2.12)] ($F = 23.019$, $p < 0.001$). HE staining results for pancreatic tissues were observed under a 200× microscope (Figure 4E−H). Fat droplets were large and partially fused in the HU and HF groups and were small in the HUHF group. Almost no fat droplets were detected in the NC group. According to the established scoring criteria, the mean pathological scores (Figure 5B and Table 1 Section B) in the HUHF group [0.77 (0.02)] were significantly lower than those in the HU group [0.98 (0.03)] and the HF group [1.03 (0.02)] but higher than that in the NC group [0.38 (0.02)] ($F = 205.108$, $p < 0.001$). There was a correlation (correlation coefficient = 0.876; $p < 0.001$) between ultrasound findings and pathology results (Figure 5C).

The mRNA and relative protein expression levels of PLA2G1B and PLA2G2A were evaluated (Table 1 Section C). The mRNA expression level of *PLA2G1B* (Figure 6A) in the HU group [5.97 (0.59)] was significantly higher than those in the HF [2.33 (0.74)], HUHF [3.66 (0.81)], and NC groups [2.44 (0.76)] ($F = 5.384$, $p = 0.004$). In contrast, the relative protein expression levels of PLA2G1B (Figure 7B) were significantly lower in the HU [0.29 (0.04)] and NC groups [0.18 (0.05)] than in the HF [0.91 (0.06)] and HUHF groups [0.84 (0.07)] ($F = 46.521$, $p < 0.001$). The mRNA expression levels of *PLA2G2A* did not differ among groups (Figure 6B) (F = 0.658, $p = 0.583$). However, the relative protein expression level of PLA2G2A (Figure 7C) was significantly higher in the HU group [0.91 (0.07)] than in the HF [0.37 (0.12)], HUHF [0.38 (0.22)], and NC groups [0.54 (0.13)] ($F = 4.880$, $p = 0.007$).
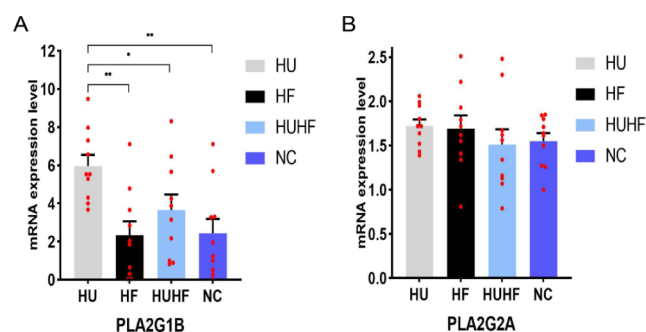
Figure 6. Analysis of mRNA expression levels. (A) mRNA expression level of *PLA2G1B* in each group. (B) mRNA expression level of *PLA2G2A* in each group. PLA2G1B: phospholipase A2 group IB; PLA2G2A: phospholipase A2 group IIA; HU: high uric acid; HF: high fat; HUHF: high uric acid and high fat; NC: normal control. * $p < 0.05$; ** $p < 0.01$; *** $p < 0.001$.

■ DISCUSSION

Mice body weights in the HF group were significantly higher than those in the other three groups, consistent with the established relationship between a high-fat diet and the accumulation of body weights.[31,39] However, our experiment showed that uric acid was not positively correlated with serum lipids. This finding is inconsistent with those of some previous studies, which suggested that hyperuricemia can lead to elevated lipid levels and ectopic fat deposition.[30,31,32] However, uric acid has excellent antioxidant properties at low concentrations[19−23] and only functions as a pro-oxidant at high concentrations, which is harmful to the body.[40] Similar studies have shown that uric acid plays dual roles; for example, moderate elevations in SUA at low concentrations can improve diabetic complications[17] and can lead to the aggravation of diabetes. The SUA level has a "J" shaped relationship with the risk of death associated with prostate cancer[18] with the risk of death decreasing and then increasing as SUA levels rise. High levels of SUA are protective against neurological disorders, such as Parkinson's disease, whereas low levels are harmful.[23−26]

Mice in the HU group had the highest SUA level (close to 100 mol/L), whereas mice in the HF group had the lowest SUA level (approximately 40 μmol/L). The SUA levels of the mice in the HUHF, and NC groups were similar (approximately 60 μmol/L). This also proved that SUA levels were relatively low in this experiment. Lipids data suggested that SUA was neither positively correlated with TC, TG, or LDL nor was it inversely correlated with HDL. This is another indication that SUA and lipid levels are not linearly correlated. Therefore, we have a conjecture that it could be more possibly a J-shaped curve such

as above-mentioned prostate cancer. Our results are possibly a descending branch of the J-shaped curve, because the mice in our study had low uric acid (less than 100 μmol/L).

The pathological scores obtained using the modified scoring method for PS were in good agreement with the ultrasound images, indicating that high-frequency ultrasonography can be used as an effective diagnostic method for PS in mice. Although pathological examination is the most accurate method for diagnosing PS, obtaining pathological results often requires the execution of animals, preventing observations of subsequent changes in the animals. Observing pancreatic lesions at different times would require additional animals, requiring large sample sizes. The extent of PS can be reflected by ultrasound, as evidenced by the good agreement between ultrasound and pathology findings. Ultrasound is a noninvasive examination that can be repeated for the same animal at different times, enabling analyses of the dynamic changes in the PS without the need for additional groups. The fPEI based on images of the mouse pancreas acquired by high-frequency ultrasonography suggests that PS was less severe in mice on the high uric acid and high-fat diet than in mice on the high uric acid or high-fat diet alone; however, it was still more severe than that in mice fed the normal diet. This further demonstrates and complements the conjecture that SUA inhibits fat accumulation or promotes lipolysis when its concentration elevated at lower ones. Pancreatic pathology showed large and partially fused fat droplets in the HU and HF groups, whereas small fat droplets were found in the HUHF group. No fat droplets were observed in the control group. This pathological finding further verified the conjecture.

PLA2G1B can lead to obesity, insulin resistance, and hyperlipidemia.[34] The results showed that the mRNA expression level of *PLA2G1B* was higher, and the relative protein expression of PLA2G1B was lower in the HU group than in the HF group. These results confirm the conjecture that low concentrations of SUA can inhibit fat accumulation. Therefore, PLA2G1B protein expression was lower in the HU group, whereas the mRNA expression level was elevated possibly due to self-regulation[41] such as negative feedback. In addition, the protein expression level of PLA2G1B was positively correlated with a high-fat diet. However, PLA2G2A expression patterns were the opposite of those for PLA2G1B.[36,42] The relative protein expression of PLA2G2A was higher in the HU group in this study, consistent with the results of previous studies.[35,36] However, there were no differences in the mRNA expression level of *PLA2G2A* among groups, suggesting that other genes may be involved in the regulation of PLA2G2A.
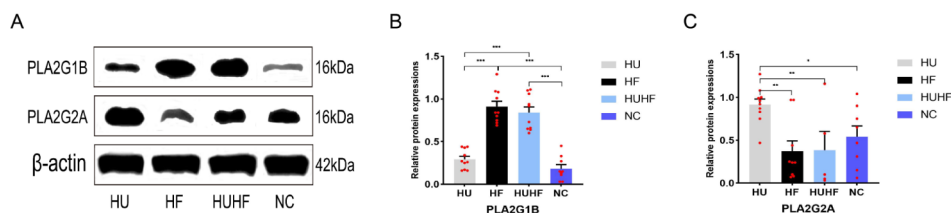

Figure 7. Analysis of relative protein expression levels. (A) Relative protein expression levels of PLA2G1B, PLA2G2A, and β-actin. (B) Gray values of relative protein expression of PLA2G1B in each group ($n = 9$ for NC and $n = 10$ for others). (C) The gray value of relative protein expression of PLA2G2A in each group ($n = 10$ for HU, $n = 9$ for HF, $n = 5$ for HUHF, $n = 8$ for NC). PLA2G1B: phospholipase A2 group IB; PLA2G2A: phospholipase A2 group IIA; HU: high uric acid; HF: high fat; HUHF: high uric acid and high fat; NC: normal control. * $p < 0.05$; ** $p < 0.01$; *** $p < 0.001$.

Most studies have shown[28−31,43] that there is a degree of interaction between SUA and lipids and that uric acid has negative health effects. However, the results in this study revealed that low concentrations of SUA inhibit fat accumulation. This suggests that there may be a nonlinear relationship between SUA and lipids, with lipids decreasing as SUA rises at low concentrations and increasing as it rises past a threshold level. Thus, uric acid can be beneficial under some conditions.

This study had some limitations. Some of the results obtained in this study are inconsistent with previous studies; therefore, more experiments are needed to verify these findings. Uricase in mice inhibits the elevation of uric levels. Therefore, uricase knockout can be used to obtain a high uric acid concentration in mice and further verify the study results. In addition, one method of stratification of SUA concentrations can be used in the future to further discover the association between SUA and lipids in different stratification.

In conclusion, low concentrations of SUA increase can inhibit fat accumulation and further inhibit PS and regulate it via the glycerophospholipid metabolic pathway. The present study suggests that an appropriate increase in SUA at low concentrations would be beneficial to fat metabolism.

ASSOCIATED CONTENT

Data Availability Statement
The data sets used and/or analyzed during the current study are available from the corresponding author on reasonable request.

Supporting Information
The Supporting Information is available free of charge at https://pubs.acs.org/doi/10.1021/acsomega.3c08874.

> The ingredient list for the common feed (Figure S1); the pancreatic steatosis rating scale (Table S1); the primer sequences of PCR experiment (Table S2) (PDF)

AUTHOR INFORMATION

Corresponding Authors
Guorong Lyu − *Department of Ultrasonography, Second Affiliated Hospital of Fujian Medical University, Quanzhou 362002, China; Department of Medicine, Quanzhou Medical College, Quanzhou 362002, China;* Email: lgr_feus@sina.com

Shilin Li − *Department of Ultrasonography, Second Affiliated Hospital of Fujian Medical University, Quanzhou 362002, China;* orcid.org/0000-0003-1195-2245; Email: lslqz@fjmu.edu.cn

Authors
Yang Xiao − *Department of Ultrasonography, Second Affiliated Hospital of Fujian Medical University, Quanzhou 362002, China*

Lina Han − *Department of Ultrasonography, Second Affiliated Hospital of Fujian Medical University, Quanzhou 362002, China*

Han Wang − *Department of Ultrasonography, Second Affiliated Hospital of Fujian Medical University, Quanzhou 362002, China*

Helin Ke − *Department of Ultrasonography, Second Affiliated Hospital of Fujian Medical University, Quanzhou 362002, China*

Shaodan Xu − *Department of Ultrasonography, Second Affiliated Hospital of Fujian Medical University, Quanzhou 362002, China*

Zhibin Huang − *Department of Ultrasonography, Second Affiliated Hospital of Fujian Medical University, Quanzhou 362002, China*

Complete contact information is available at:
https://pubs.acs.org/10.1021/acsomega.3c08874

Author Contributions
The original draft of the manuscript was written by Y.X. The data for the study were collected by L.H. and H.W. The data curation and formal analysis were performed by Y.X. and S.L. The animal rearing was performed by H.K., S.X., and Z.H. The revision of the manuscript was done by Y.X., G.L., and S.L. The funding acquisition was performed by S.L. All authors read and approved the final manuscript.

Notes
This study was conducted in full conformance with the principles of the Declaration of Helsinki, and the animal study protocol was approved by the Ethics Committee of the Second Affiliated Hospital of Fujian Medical University (protocol code 231 and date of approval 2022).
The authors declare no competing financial interest.

ACKNOWLEDGMENTS

ABBREVIATIONS

SUA	serum uric acid
PEI	pancreatic echo intensity
PS	pancreatic steatosis
PLA2G1B	phospholipase A2 group IB
PLA2G2A	phospholipase A2 group IIA
HU	high uric acid
HF	high fat
HUHF	high uric acid and high fat
NC	normal control
qRT-PCR	quantitative reverse transcriptase-polymerase chain reaction
TG	triglyceride
TC	total cholesterol
HDL	high-density lipoprotein
LDL	low-density lipoprotein

REFERENCES

(1) GBD 2015 Obesity Collaborators. Health effects of overweight and obesity in 195 countries over 25 years *N. Engl. J. Med.* **2017** 377 1 1327

(2) Brown, O.-I.; Drozd, M.; McGowan, H.; Giannoudi, M.; Conning-Rowland, M.; Gierula, J.; Straw, S.; Wheatcroft, S.-B.; Bridge, K.; Roberts, L.-D. Relationship among diabetes, obesity, and cardiovascular disease phenotypes: A UK Biobank cohort study. *Diabetes Care* **2023**, 46 (8), 1531−1540.

(3) Nguyen, H.-L.; Geukens, T.; Maetens, M.; Aparicio, S.; Bassez, A.; Borg, A. Obesity-associated changes in molecular biology of primary breast cancer. *Nat. Commun.* **2023**, 14 (1), 4418.

(4) Cao, M.-J.; Wu, W.-J.; Chen, J.-W.; Fang, X.-M.; Ren, Y.; Zhu, X.-W.; Cheng, H.-Y.; Tang, Q.-F. Quantification of ectopic fat storage in the liver and pancreas using six-point Dixon MRI and its association with insulin sensitivity and β-cell function in patients with central obesity. *Eur. Radiol.* **2023**, *33*, 9213−9222.

(5) Catanzaro, R.; Cuffari, B.; Italia, A.; Marotta, F. Exploring the metabolic syndrome: Nonalcoholic fatty pancreas disease. *World J. Gastroenterol.* **2016**, *22* (34), 7660−7675.

(6) Lu, W.; Li, X.; Luo, Y. FGF21 in obesity and cancer: New insights. *Cancer Lett.* **2021**, *499*, 5−13.

(7) Alempijevic, T.; Dragasevic, S.; Zec, S.; Popovic, D.; Milosavljevic, T. Non-alcoholic fatty pancreas disease. *Postgrad. Med. J.* **2017**, *93* (1098), 226−230.

(8) Ko, J.; Al-Ani, Z.; Long, K.; Tarrant, C.; Skudder-Hill, L.; Petrov, M.-S. Intrapancreatic, Liver, and Skeletal Muscle Fat Depositions in First Attack of Acute Pancreatitis Versus Health. *Am. J. Gastroenterol.* **2022**, *117* (10), 1693−1701.

(9) Sotoudehmanesh, R.; Tahmasbi, A.; Sadeghi, A.; Hosseini, H.; Mohamadnejad, M. The prevalence of nonalcoholic fatty pancreas by endoscopic ultrasonography. *Pancreas* **2019**, *48* (9), 1220−1224.

(10) Sepe, P.-S.; Ohri, A.; Sanaka, S.; Berzin, T.-M.; Sekhon, S.; Bennett, G.; Mehta, G.; Chuttani, R.; Kane, R.; Pleskow, D. A prospective evaluation of fatty pancreas by using EUS. *Gastrointest. Endosc.* **2011**, *73* (5), 987−993.

(11) Han, Y.; Cao, Y.; Han, X.; Di, H.; Yin, Y.; Wu, J.; Zhang, Y.; Zeng, X. Hyperuricemia and gout increased the risk of long-term mortality in patients with heart failure: Insights from the National Health and Nutrition Examination Survey. *J. Transl. Med.* **2023**, *21* (1), 463.

(12) Nardin, C.; Sponchiado, A.; Raggi, D.; Faggin, E.; Martini, E.; Pagliara, V.; Callegari, E.; Caberlotto, L.; Plebani, M.; Pauletto, P. Serum uric acid levels and the risk of recurrent venous thromboembolism. *J. Thromb. Haemostasis* **2021**, *19* (1), 194−201.

(13) Sultan, A.-A.; Muller, S.; Whittle, R.; Roddy, E.; Mallen, C.; Clarson, L. Venous thromboembolism in patients with gout and the impact of hospital admission, disease duration and urate-lowering therapy. *CMAJ* **2019**, *191* (22), No. E597−E603.

(14) Ji, L.; Shu, P. A Mendelian randomization study of serum uric acid with the risk of venous thromboembolism. *Arthritis Res. Ther.* **2023**, *25* (1), 122.

(15) Volpe, A.; Ye, C.; Hanley, A.-J.; Connelly, P.-W.; Zinman, B.; Retnakaran, R. Changes Over Time in Uric Acid in Relation to Changes in Insulin Sensitivity, Beta-Cell Function, and Glycemia. *J. Clin. Endocrinol. Metab.* **2020**, *105* (3), No. e651−9.

(16) Lu, J.; He, Y.; Cui, L.; Xing, X.; Liu, Z.; Li, X.; Zhang, H.; Li, H.; Sun, W.; Ji, A. Hyperuricemia predisposes to the onset of diabetes via promoting pancreatic β-cell death in uricase-deficient male mice. *Diabetes* **2020**, *69* (6), 1149−1163.

(17) Dai, Y.; Jiang, Y.; Zhang, L.; Qiu, X.; Gu, H.; Jiang, Y.; Meng, X.; Li, Z.; Wang, Y. Moderate elevation of serum uric acid levels improves short-term functional outcomes of ischemic stroke in patients with type 2 diabetes mellitus. *BMC Geriatr.* **2023**, *23* (1), 445.

(18) Lee, Y.-H.-A.; Chan, J.-S.-K.; Leung, C.-H.; Hui, J.-M.-H.; Dee, E.-C.; Ng, K.; Liu, K.; Liu, T.; Tse, G.; Ng, C.-F. Association between serum uric acid and prostate cancer mortality in androgen deprivation therapy: A population-based cohort study. *Cancer Med.* **2023**, *12* (16), 17056−17060.

(19) Dalbeth, N.; Choi, H. K.; Joosten, L. A. B.; Khanna, P. P.; Matsuo, H.; Perez-Ruiz, F.; Stamp, L. K. Gout. *Nat. Rev.: Dis. Primers* **2019**, *5* (10287), 69.

(20) Ames, B.-N.; Cathcart, R.; Schwiers, E.; Hochstein, P. Uric acid provides an antioxidant defense in humans against oxidant- and radical-caused aging and cancer: A hypothesis. *Proc. Natl. Acad. Sci. U. S. A.* **1981**, *78* (11), 6858−6862.

(21) Wang, M.; Wu, J.; Jiao, H.; Oluwabiyi, C.; Li, H.; Zhao, J.; Zhou, Y.; Wang, X.; Lin, H. Enterocyte synthesizes and secrets uric acid as antioxidant to protect against oxidative stress via the involvement of Nrf pathway. *Free Radical Biol. Med.* **2022**, *179*, 95−108.

(22) Fabbrini, E.; Serafini, M.; Colic Baric, I.; Hazen, S.-L.; Klein, S. Effect of plasma uric acid on antioxidant capacity, oxidative stress, and insulin sensitivity in obese subjects. *Diabetes* **2014**, *63* (3), 976−981.

(23) Seifar, F.; Dinasarapu, A.-R.; Jinnah, H.-A. Uric acid in Parkinson's disease: What is the connection? *Mov. Disord.* **2022**, *37* (11), 2173−2183.

(24) van Wamelen, D.-J.; Taddei, R.-N.; Calvano, A.; Titova, N.; Leta, V.; Shtuchniy, I.; Jenner, P.; Martinez-Martin, P.; Katunina, E.; Chaudhuri, K.-R. Serum Uric Acid Levels and Non-Motor Symptoms in Parkinson's Disease. *J. Parkinson's Dis.* **2020**, *10* (3), 1003−1010.

(25) Constantin, I.-M.; Voruz, P.; Péron, J.-A. Moderating effects of uric acid and sex on cognition and psychiatric symptoms in asymmetric Parkinson's disease. *Biol. Sex Differ.* **2023**, *14* (1), 26.

(26) Gao, X.; O'Reilly, É.-J.; Schwarzschild, M.-A.; Ascherio, A. Prospective study of plasma urate and risk of Parkinson disease in men and women. *Neurology* **2016**, *86* (6), 520−526.

(27) Cui, J.; Hong, P.; Li, Z.; Lin, J.; Wu, X.; Nie, K.; Zhang, X.; Wan, J. Chloroquine inhibits NLRP3 inflammasomes activation and alleviates renal fibrosis in mouse model of hyperuricemic nephropathy with aggravation by a high-fat-diet. *Int. Immunopharmacol.* **2023**, *120*, 110353.

(28) Harmon, D.-B.; Mandler, W.-K.; Sipula, I.-J.; Dedousis, N.; Lewis, S.-E.; Eckels, J.-T.; Du, J.; Wang, Y.; Huckestein, B.-R.; Pagano, P.-J. Hepatocyte-Specific Ablation or Whole-Body Inhibition of Xanthine Oxidoreductase in Mice Corrects Obesity-Induced Systemic Hyperuricemia Without Improving Metabolic Abnormalities. *Diabetes* **2019**, *68* (6), 1221−1229.

(29) Zhang, Y.; Zhang, M.; Yu, X.; Wei, F.; Chen, C.; Zhang, K.; Feng, S.; Wang, Y.; Li, W.-D. Association of hypertension and hyper-triglyceridemia on incident hyperuricemia: An 8-year prospective cohort study. *J. Transl. Med.* **2020**, *18* (1), 409.

(30) Wang, X.; Zhong, S.; Guo, X. The associations between fasting glucose, lipids and uric acid levels strengthen with the decile of uric acid increase and differ by sex. *Nutr., Metab. Cardiovasc. Dis.* **2022**, *32* (12), 2786−2793.

(31) Lee, M.-J.; Khang, A.-R.; Kang, Y.-H.; Yun, M.-S.; Yi, D. Synergistic interaction between hyperuricemia and abdominal obesity as a risk factor for metabolic syndrome components in Korean population. *Diabetes Metab. J.* **2022**, *46* (5), 756−766.

(32) Wei, X.; Jia, X.; Liu, R.; Zhang, S.; Liu, S.; An, J.; Zhou, L.; Zhang, Y.; Mo, Y.; Li, X. Metabolic pathway analysis of hyperuricaemia patients with hyperlipidaemia based on high-throughput mass spectrometry: A case−control study. *Lipids Health Dis.* **2022**, *21* (1), 151.

(33) Lyu, S.; Ding, R.; Liu, P.; OuYang, H.; Feng, Y.; Rao, Y.; Yang, S. LC-MS analysis of serum for the metabolomic investigation of the effects of Pulchinenoside b4 administration in monosodium urate crystal-induced gouty arthritis rat model. *Molecules* **2019**, *24* (17), 3161.

(34) Hollie, N.-I.; Konaniah, E.-S.; Goodin, C.; Hui, D.-Y. Group 1B phospholipase A₂ inactivation suppresses atherosclerosis and metabolic diseases in LDL receptor-deficient mice. *Atherosclerosis* **2014**, *234* (2), 377−380.

(35) Kuefner, M.-S.; Deng, X.; Stephenson, E.-J.; Pham, K.; Park, E.-A. Secretory phospholipase A2 group IIA enhances the metabolic rate and increases glucose utilization in response to thyroid hormone. *FASEB J.* **2019**, *33* (1), 738−749.

(36) Kuefner, M.-S.; Stephenson, E.; Savikj, M.; Smallwood, H.-S.; Dong, Q.; Payré, C.; Lambeau, G.; Park, E.-A. Group IIA secreted phospholipase A2 (PLA2G2A) augments adipose tissue thermogenesis. *FASEB J.* **2021**, *35* (10), No. e21881.

(37) Lefkowitch, J.-H. Morphology of alcoholic liver disease. *Clin. Liver Dis.* **2005**, *9* (1), 37−53.

(38) Yerian, L. Histopathological evaluation of fatty and alcoholic liver diseases. *J. Dig. Dis.* **2011**, *12* (1), 17−24.

(39) Han, C.-Y.; Kang, I.; Harten, I.-A.; Gebe, J.-A.; Chan, C.-K.; Omer, M.; Alonge, K.-M.; den Hartigh, L.-J.; Gomes Kjerulf, D.; Goodspeed, L. Adipocyte-derived versican and macrophage-derived biglycan control adipose tissue inflammation in obesity. *Cell Rep.* **2020**, *31* (13), 107818.

(40) So, A.; Thorens, B. Uric acid transport and disease. *J. Clin. Invest.* **2010**, *120* (6), 1791−1799.

(41) Liang, W.-J.; Zhang, G.; Luo, H.-S.; Liang, L.-X.; Huang, D.; Zhang, F.-C. Tryptase and Protease-Activated Receptor 2 Expression Levels in Irritable Bowel Syndrome. *Gut Liver* **2016**, *10* (3), 382−390.

(42) Schewe, M.; Franken, P.-F.; Sacchetti, A.; Schmitt, M.; Joosten, R.; Böttcher, R.; van Royen, M.-E.; Jeammet, L.; Payré, C.; Scott, P.-M. Secreted phospholipases A2 are intestinal stem cell niche factors with distinct roles in homeostasis, inflammation, and cancer. *Cell Stem Cell* **2016**, *19* (1), 38−51.

(43) Hu, Y.; Li, J.; Yin, C.; Xu, L.; Li, S.; Chen, Y.; Wang, Y.; Cheng, Z.; Bai, Y. Mediating effect of metabolic diseases on the relationship between hyperuricemia and coronary heart disease. *Nutr. Metab. Cardiovasc. Dis* **2023**, *33* (2), 315−322.